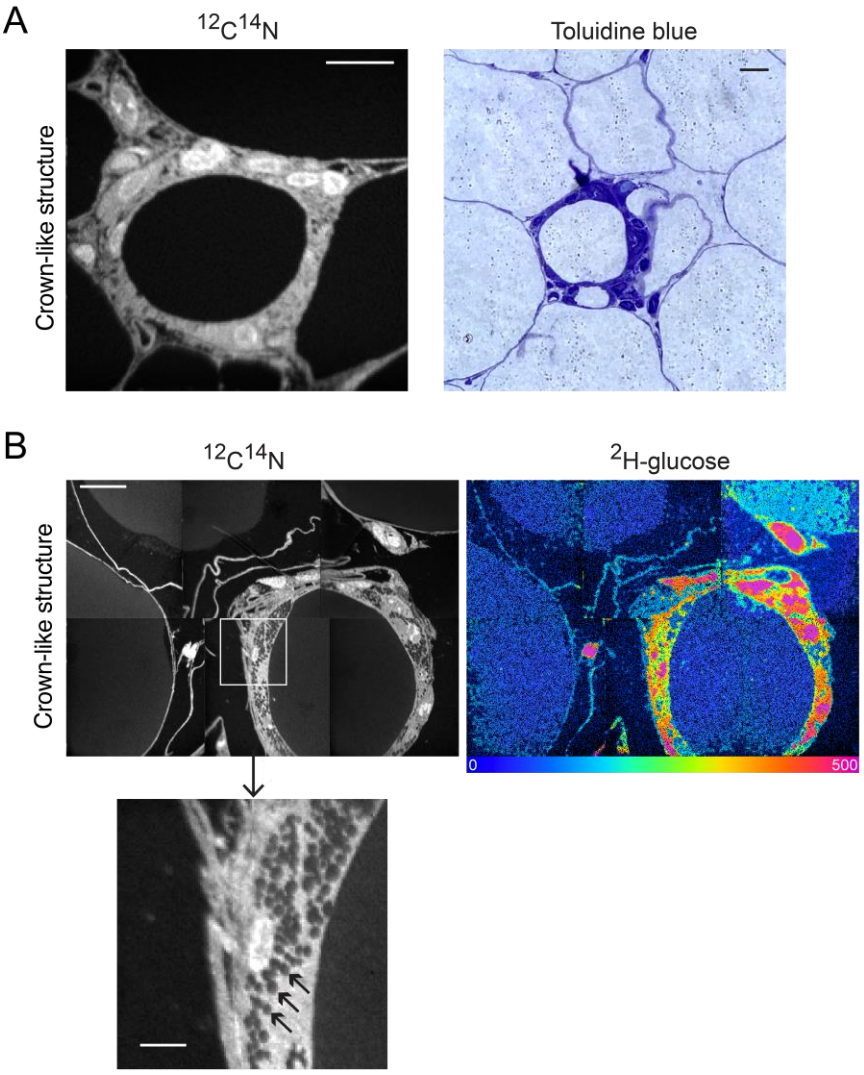

Figure S1. Identification of "crown-like structures" with Multi-Isotope Imaging Mass Spectrometry (MIMS).

A. Crown-like structure (CLS) shown in Figure 1 with Toluidine blue staining of adjacent section several microns removed in the z-axis. Scale bars=10μm.

B. Representative MIMS imaging of murine AT after labeling with ^{2}H-glucose. In this mosaic image, adjacent imaging fields are stitched together to capture a stereotypical CLS. There is intense ^{2}H-glucose labeling of the cells that comprise the "crown," consistent with glucose avid inflammatory cells. In this particular CLS, several of the cells that comprise the crown have an appearance similar to atherosclerotic foam cells with numerous small intracellular droplets (arrows, inset). Scale (top) = 20μm; scale (inset) = 5μm.

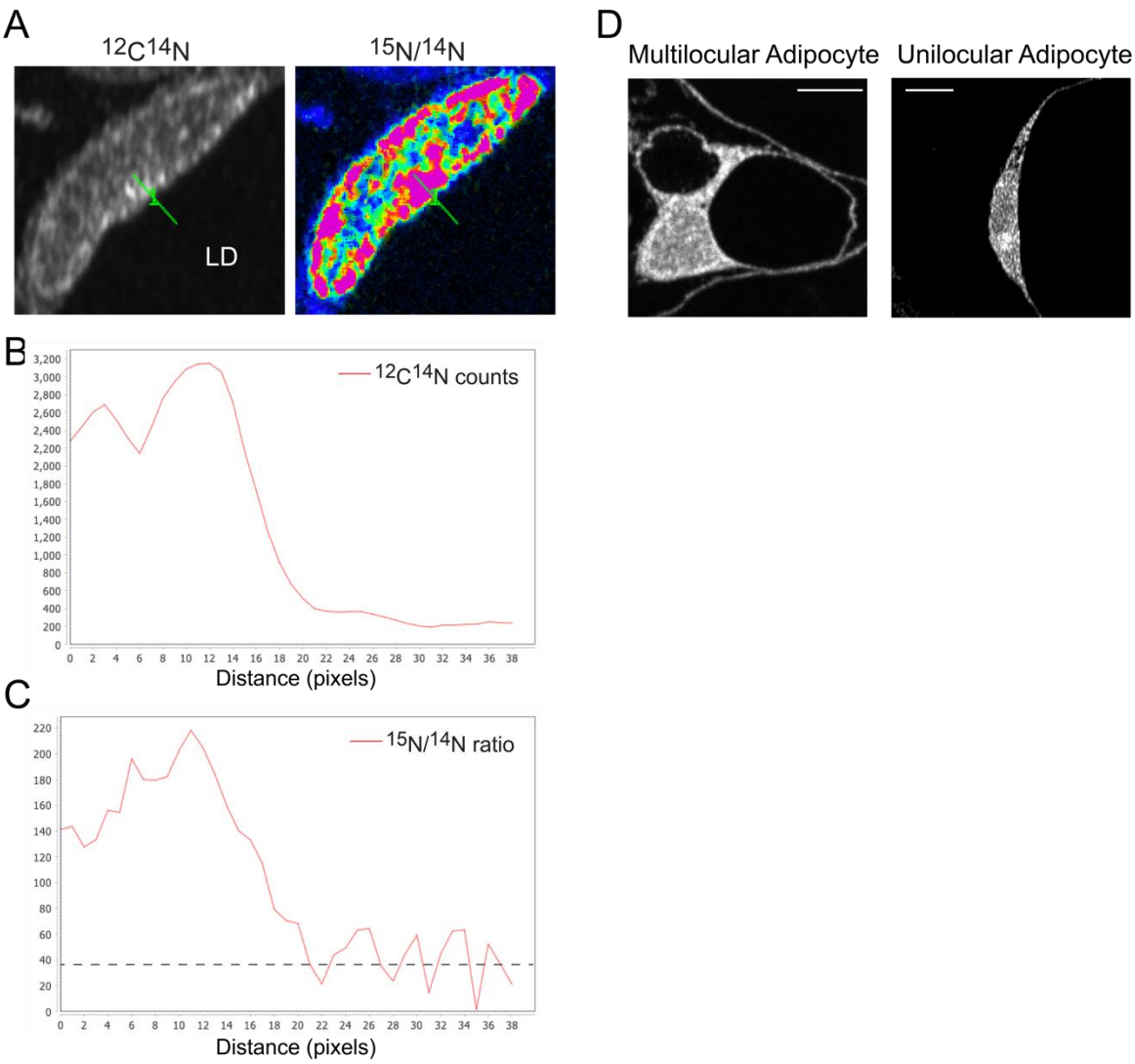

Figure S2. Identification of ^{15}N-thymidine labeled adipocytes with Multi-Isotope Imaging Mass Spectrometry (MIMS).

A. Representative ^{15}N-thymidine labeled adipocyte nucleus adjacent to dominant lipid droplet (LD). The linear green region of interest was selected in the OpenMIMS software in order to graph the quantitative relationship between the CN signal and the ^{15}N/^{14}N ratio as shown in B and C. The CN signal in the lipid droplet proper is negligible (appears black) because neutral lipid and the embedding resin is nitrogen poor.

B. Line profile of CN counts for the linear green region of interest (ROI) shown in A. As seen visually in A, there is a marked drop off at the approximate midpoint of the line in CN counts corresponding to the transition from the nucleus to the lipid droplet region of the cell.

C. Line profile of the ^{15}N/^{14}N ratio for the linear green region of interest (ROI) shown in A. The ratio (y-axis) is expressed x10^4, which is the default of the OpenMIMS software. The natural background of ^{15}N is 0.0037, which by default is expressed as 37 in the OpenMIMS software (dashed line=natural background). The drop in ^{15}N-labeling occurs at the same point as CN (B), which is indicative of the nucleus to

lipid droplet transition. This demonstrates the close association of the ^{15}N-labeled nucleus with the adipocyte-defining lipid droplet.

D. Multilocular adipocyte shown in Figure 1 and representative unilocular adipocyte. In the analyses of the ^{15}N-thymidine labeled adipocytes after an 8-week labeling protocol, the majority of cells displayed features consistent with a classical white adipocyte with a single dominant lipid droplet (unilocular), even though the putative new adipocytes identified by this labeling protocol are smaller relative to older unlabeled adipocytes(1). Approximately 10% of the ^{15}N-labeled adipocytes demonstrated the multi-locular appearance, which is consistent with a more immature adipocyte. Scale = 5μm.

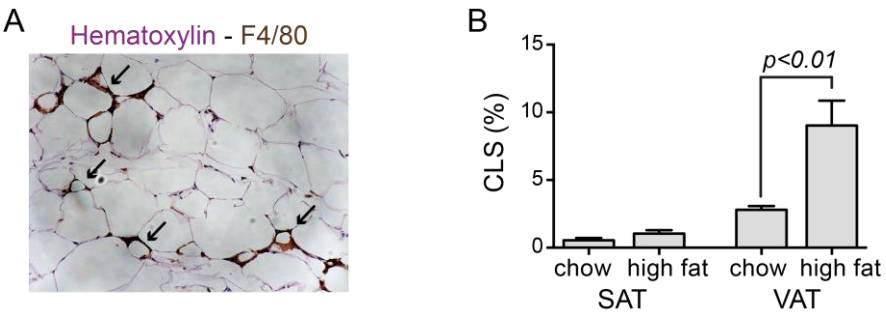

Figure S3. Adipocyte death with diet-induced obesity. C57Bl6 mice were administered high fat or chow control diet for 8 weeks, starting at 10 weeks of age.

A. Representative immunohistochemical assessment of “crown-like structures (arrows), which are putative dead adipocytes.
B. Quantification of CLS frequency in iWAT and gWAT.

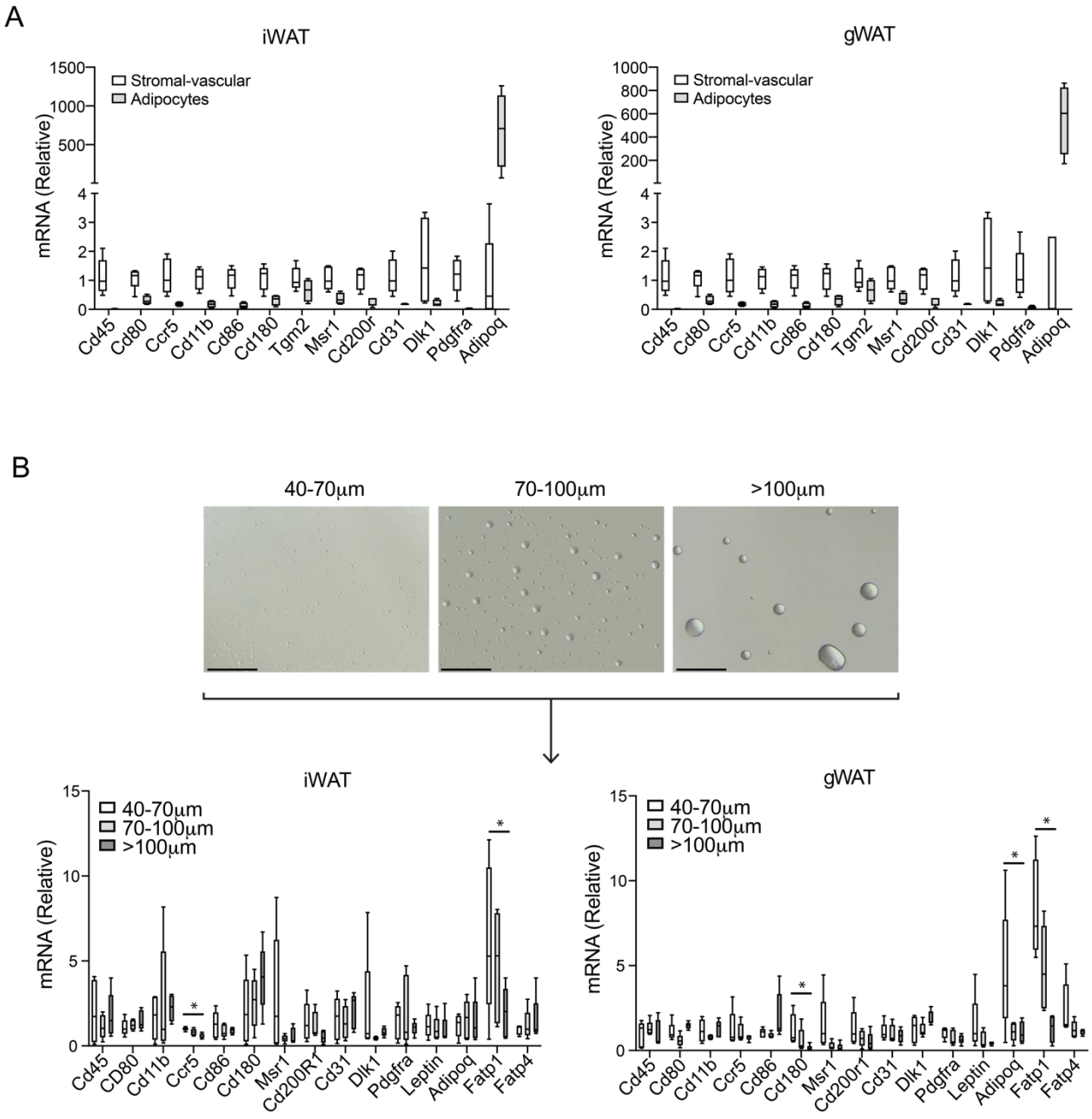

Figure S4. Isolation of adipocyte fractions.

A. qPCR analyses of immune cell, endothelial, preadipocyte, and adipocyte markers in stromal-vascular and adipocyte fractions.

B. Top: Representative brightfield images of adipocyte fractions after adipose tissue digestion and serial filtration. Scale = 200μm. Bottom: qPCR analyses of immune cell, endothelial, preadipocyte, and adipocyte markers in adipocyte fractions as a function of size. Ccr5 (iWAT), Cd180, Adipoq (gWAT), and Fatp1 (both depots) demonstrated a decline as a function of increasing size (ANOVA, test for linear trend).

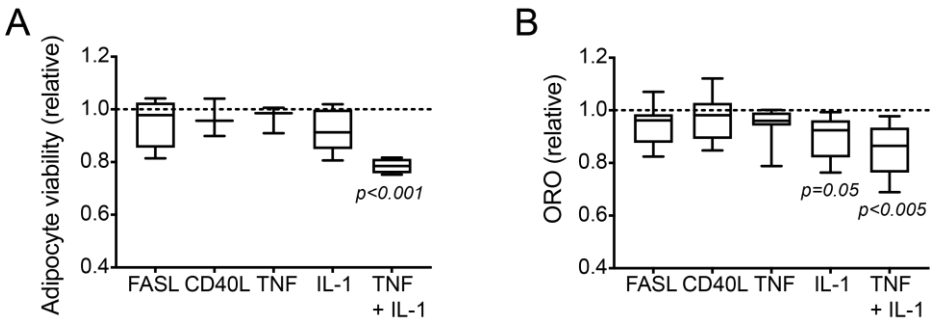

Figure S5. Inflammatory cytokine mediated death of 3T3L1-derived adipocytes.

A. Summary of experiments assessing adipocyte viability after exposure to death ligands. Viability assayed by MTT assay after exposure to death ligands. n=3-5 biological replicate experiments were normalized to vehicle control (dashed line). Adipocytes derived from differentiation of 3T3L1 cells.

B. Summary of experiments assessing adipocyte viability after exposure to death ligands. Viability assayed by ORO staining, extraction, and reading at OD=520. Data are normalized to vehicle control (n=6-8 biological replicate experiments). Adipocytes derived from differentiation of 3T3L1 cells.

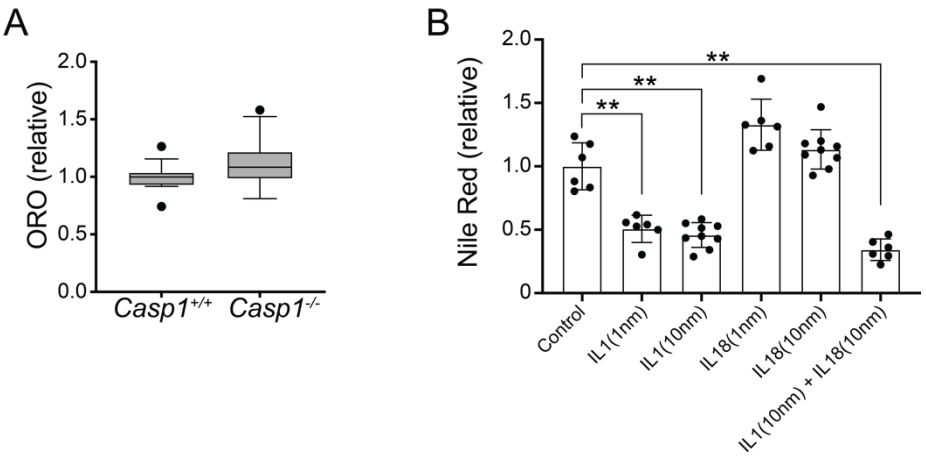

Figure S6. Caspase 1 and adipogenesis *in vitro.*

A. Tukey box plots of ORO staining after adipogenic differentiation of primary adipocyte progenitor cells isolated from *Casp1*$^{+/+}$ or *Casp*$^{-/-}$ mice. N=16-18, normalized to wild-type. The trend in the knockout cells did not reach significance (p=0.06, Mann-Whitney test).

B. 3T3L1 cells undergoing adipogenic differentiation were treated with cytokines activated by Caspase 1, IL-1 and IL-18. Adipogenesis was assessed by Nile Red staining and normalized to control. IL-1 attenuated adipogenesis. **p<0.001

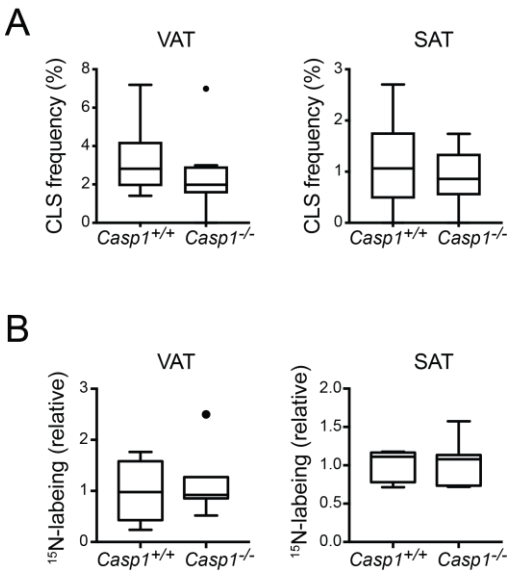

Figure S7. Adipocyte death and birth with Caspase-1 loss of function in diet-induced obesity.

A. No significant difference in CLS frequency (adipocyte death) was observed in *Casp1*$^{-/-}$ mice relative to wild-type mice after high fat feeding.

B. No significant difference in adipogenesis, as assayed by ^{15}N-thymidine labeling of adipocytes in *Casp1*$^{-/-}$ mice after high fat feeding.

Reference

1. Kim SM, Lun M, Wang M, Senyo SE, Guillermier C, Patwari P, Steinhauser ML: Loss of white adipose hyperplastic potential is associated with enhanced susceptibility to insulin resistance. Cell Metab 2014;20:1049-1058